Vol. 13 (2020) *Acta Physica Polonica B Proceedings Supplement* No 1

# RECENT JPAC ANALYSIS OF $\eta^{(\prime)}\pi$ RESONANCES*

A. Rodas

Departamento de Física Teórica and IPARCOS
Universidad Complutense de Madrid, 28040 Madrid, Spain

*(Received June 24, 2019)*

In this paper, we review a recent analysis of the $\eta^{(\prime)}\pi$ system using COMPASS data. The extracted relative phases and intensities are fitted with a coupled-channel formalism fulfilling both unitarity and analyticity. As a result, a robust extraction of a single isolated exotic $\pi_1(1600)$ is provided, decaying to both $\eta^{(\prime)}\pi$ final states, together with the determination of the resonance parameters of the $a_2(1320)$ and $a_2'(1700)$. No statistical significance for a second exotic state is found.

DOI:10.5506/APhysPolBSupp.13.45

## 1. Introduction

Describing the hadron structure in terms of quarks and gluons is the key to our understanding of Quantum Chromodynamics (QCD). Even though most of the observed mesons can be classified as $q\bar{q}$ states, QCD has a much richer spectrum [1]. Several QCD-based models predict states with explicit gluonic degrees of freedom, also known as hybrids [2], which have also been supported by Lattice QCD calculations [3]. A single state with the following quantum numbers $J^{PC}(I^G) = 1^{-+}(1^-)$ is expected below 2 GeV. Nevertheless, experiments claimed two different states to exist, the first $\pi_1(1400)$ decaying into $\eta\pi$, and the second $\pi_1(1600)$ decaying into $\rho\pi$ and $\eta'\pi$ channels. Recent high statistic analyses coming from COMPASS confirmed a peak in both $\rho\pi$ and $\eta'\pi$ at around 1.6 GeV [4, 5] and another structure in $\eta\pi$, close to 1.4 GeV [6]. However, no coupled-channel analysis was performed by experimental collaborations.

In [7], we studied the spectrum of both the $\eta^{(\prime)}\pi$ $D$- and $P$-waves from the COMPASS data with a coupled-channel formalism, extending the method in our previous analysis [8]. As a result, the existence of a single $\pi_1$ pole decaying to both channels is obtained, together with the determination of the resonance parameters of the $a_2(1320)$ and $a_2'(1700)$.

* Presented at "Excited QCD 2019", Schladming, Austria, January 30–February 3, 2019.

## 2. Data and model description

We analyzed the data of both $P$ and $D$ partial waves from the COMPASS Collaboration [6], extracted from a mass-independent analysis of $\pi p \to \eta^{(\prime)}\pi p$, where the energy of the pion beam in the lab frame is 191 GeV. Due to this highly energetic beam, most of the events are produced in the forward direction, with around 90% lying close to the lower limit of the measured transferred momentum squared $-t_1 \in [0.1, 1]$ GeV$^2$. The data is extracted up to 3 GeV, however, there are several reasons [7] why we decided to discard all data points above roughly 2 GeV, however, it is worth noticing that all relevant resonances appear far below that energy region.

Recently, COMPASS has published the $3\pi$ partial-wave analysis [4], including the exotic $1^{-+}$ partial wave in the $\rho\pi$ channel. Nonetheless, the extraction of the resonance pole in this channel is hindered by the Deck mechanism [9, 10]. It is worth noticing, as discussed in [8], that neglecting additional channels does not affect the pole position in cases like the one we are studying, so that we will only consider $\eta^{(\prime)}\pi$ channels.

Due to the forward nature of the $\pi p \to \eta^{(\prime)}\pi p$ process, it is Pomeron ($\mathbb{P}$) dominated at high energies, which allows us to factorize the $\pi\mathbb{P} \to \eta^{(\prime)}\pi$ process. It resembles a helicity partial wave amplitude $a_i^J(s)$ for fixed $t_1$, with $i = \eta^{(\prime)}\pi$ the final state, $J$ the angular momentum of the final state and $s$ its invariant mass squared. The Pomeron must be a spin-one particle in order to explain the approximately constant hadron cross sections at high energies. Taking into account the fact that both angular momentum projections $M = \pm 1$ are related through parity, we drop the Pomeron helicity index. We finally fixed the transferred momentum to $t_{\text{eff}} = -0.1$ GeV$^2$ for simplicity, although it would be varied to estimate its systematic effect.

We parameterize the amplitudes following the coupled-channel $N/D$ formalism

$$a_i^J(s) = q^{J-1} p_i^J \sum_k n_k^J(s) \left[ D^J(s)^{-1} \right]_{ki} , \tag{1}$$

where $p_i = \lambda^{1/2}(s, m_{\eta^{(\prime)}}^2, m_\pi^2)/(2\sqrt{s})$ is the $\eta^{(\prime)}\pi$ momentum, $q = \lambda^{1/2}(s, m_\pi^2, t_{\text{eff}})/(2\sqrt{s})$ the $\pi$ beam momentum in the $\eta^{(\prime)}\pi$ rest frame, and $\lambda(a,b,c)$ is the Källén function. The numerator polynomials $n_k^J(s)$ incorporate exchange "forces" in the production process (left-hand cuts), and so are smooth functions of $s$ in the physical region. The $D^J(s)$ matrix contains the right-hand cuts constrained by the $s$-channel unitarity of $\eta^{(\prime)}\pi$ scattering.

We use an effective expansion in the Chebyshev polynomials for the numerators $n_k^J(s)$. A customary parameterization of the denominator is given by

$$D^J_{ki}(s) = \left[K^J(s)^{-1}\right]_{ki} - \frac{s}{\pi}\int_{s_k}^{\infty} \mathrm{d}s' \frac{\rho N^J_{ki}(s')}{s'(s'-s-i\epsilon)}\,, \tag{2}$$

where $s_k$ is the threshold in channel $k$ and

$$\rho N^J_{ki}(s') = \delta_{ki}\, \frac{\lambda^{J+1/2}\left(s', m^2_{\eta^{(\prime)}}, m^2_\pi\right)}{(s'+s_{\mathrm{L}})^{2J+1+\alpha}} \tag{3}$$

is an effective description of the left-hand cuts in $\eta^{(\prime)}\pi \to \eta^{(\prime)}\pi$ scattering, with the right kinematical features, where $s_{\mathrm{L}}$ is fixed at the hadronic scale $s_{\mathrm{L}} \sim 1$ GeV$^2$. Finally,

$$K^J_{ki}(s) = \sum_R \frac{g^{J,R}_k g^{J,R}_i}{m^2_R - s} + c^J_{ki} + d^J_{ki}\, s \tag{4}$$

with $c^J_{ki} = c^J_{ik}$ and $d^J_{ki} = d^J_{ik}$, is a standard parameterization for the K-matrix formalism. In the $D$-wave we explicitly included 2 K-matrix poles, and one single K-matrix pole in the $P$-wave. The numerator of both channels and waves is described by a third-order polynomial, and we set $\alpha = 2$ in Eq. (3). The remaining 37 parameters are fitted to data. The best fit has $\chi^2$/d.o.f. $= 162/122 = 1.3$, which, as shown in Fig. 1 is in good agreement

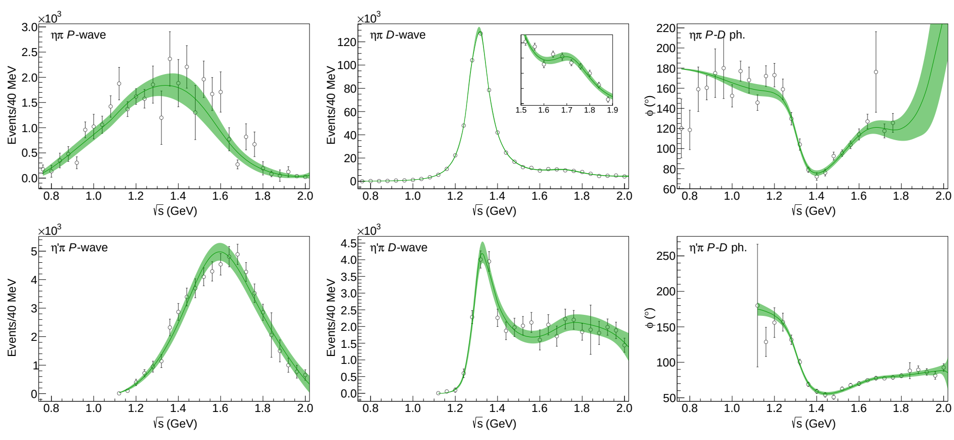


Fig. 1. (Color online) Fits to the $\eta\pi$ (upper line) and $\eta'\pi$ (lower line) data from COMPASS [6]. We shown intensities of $P$- (left), $D$-wave (center), and relative phase (right). The solid line and gray/green band show the result of the fit and the $2\sigma$ confidence level obtained by the bootstrap analysis. The errors shown are statistical only.

with data. Indeed, a single K-matrix pole in the $P$-wave correctly describes the two different peaks in the $\eta^{(\prime)}\pi$ channels. The statistical uncertainties were estimated using the bootstrap technique.

Once the best fit is obtained, the $D^J(s)$ matrix in Eq. (2) must be continued through the unitarity cut into the next Riemann sheet to determine the resonant poles. These poles $s_\mathrm{P}$ in the amplitude appear when the determinant of $D^J(s_\mathrm{P})$ vanishes. As the behavior in the real axis is driven directly by nearby poles, the ones appearing close to the unitarity cut will be identified as resonances. Even though it is customary to relate the number of K-matrix poles to the number of resonances, it is not possible to determine it using a coupled-channel formalism. Appearance of spurious poles far from the physical region is likely. However, we did identify the physical poles by testing their stability against different forms of the parameterization and data resampling. We study the resonance poles in the $m \in [1,2]$ GeV and $\Gamma \in [0,1]$ GeV region, where we define $m = \mathrm{Re}\sqrt{s_\mathrm{P}}$ and $\Gamma = -2\mathrm{Im}\sqrt{s_\mathrm{P}}$. Two poles were found in the $D$-wave, identified as the $a_2(1320)$ and $a_2'(1700)$, while a single isolated pole in the $P$-wave, the $\pi_1$, was obtained. The pole positions are shown in Fig. 2, while the resonance parameters are listed in Table I. We also performed a pure background fit for the $P$-wave, in order to estimate the significance of such resonance. The global $\chi^2$ was larger by almost two orders of magnitude when no pole was found, thus rejecting the possibility for the $P$-wave peaks to be generated by non-resonant background.

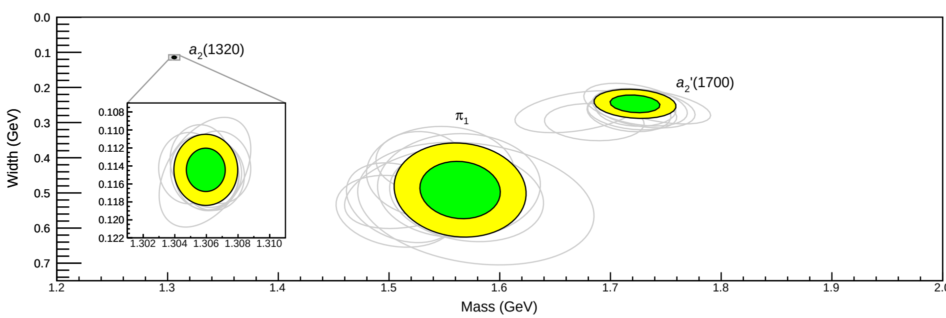


Fig. 2. (Color online) Positions of the poles identified as the $a_2(1320)$, $\pi_1$, and $a_2'(1700)$. The inner/green and outer/yellow ellipses show the $1\sigma$ and $2\sigma$ confidence levels. The gray ellipses in the background show the variations of the pole position due to the modification of the functional forms and the parameters of the model.

As is customarily done, more K-matrix poles were included to assess the significance of new possible resonances, in particular we tested the two resonance PDG scenario for the $P$-wave. Both the global and local $\chi^2$ coincide with the 1 K-matrix pole fit, on top of that, one of the two poles appears in a vast region in the complex plane depending on the initial values of the fit, with a small coupling to both partial waves, while the second one is always compatible with the single pole solution. We thus concluded that the former does not influence the real axis and is just unnecessary to describe the data, however, it changes the behavior of the phase, producing a 180° jump around 2 GeV, where no data exist.

TABLE I

Resonance parameters.

| Poles | Mass [MeV] | Width [MeV] |
|---|---|---|
| $a_2(1320)$ | $1306.0 \pm 0.8 \pm 1.3$ | $114.4 \pm 1.6 \pm 0.0$ |
| $a_2'(1700)$ | $1722 \pm 15 \pm 67$ | $247 \pm 17 \pm 63$ |
| $\pi_1$ | $1564 \pm 24 \pm 86$ | $492 \pm 54 \pm 102$ |

### 3. Systematic uncertainties

The method used to analyze the data does include some model dependencies, of which we list here the systematic uncertainties studied. Regarding the numerator, we first varied $t_{\text{eff}}$ and the order of the polynomial. For the denominator, we varied the values of the left-hand cuts $s_{\text{L}}$ and $\alpha$ in a considerable range. Finally, we modified the Chew–Mandelstam term, in order to describe the phenomenological $t$-channel exchange dominated by an intermediate particle, whose mass is considered to be of the order of 1 GeV, explicitly this term reads

$$\rho N_{ki}^{J}\left(s'\right) = \delta_{ki}\, Q_J(z_{s'})\, s'^{-\alpha} \lambda^{-1/2}\left(s', m_{\eta^{(\prime)}}^2, m_\pi^2\right) , \tag{5}$$

where $Q_J(z_s)$ is the second kind Legendre function, and $z_{s'}$ the angle of the elastic scattering. This function behaves at high energies as $s^{-\alpha}$, has a left-hand cut starting at $s = 0$, a short cut between $(s' - m_{\eta^{(\prime)}})^2$ and $(s' + m_{\eta^{(\prime)}})^2$, and an incomplete circular cut depending on the mass of the exchanged particle, considered of the hadronic scale $\simeq 1$ GeV.

The shape of the dispersive integral in Eq. (2) is of course modified, but the fit is unaffected under all these changes. The pole positions change roughly within $2\sigma$, as shown in Fig. 2, and the systematic uncertainties are listed in Table I. No statistical significance of a second exotic state was found.

### 4. Summary

A first coupled channel analysis of the $\eta^{(\prime)}\pi$ system measured at COMPASS [6] is presented by means of a K-matrix formula constrained by unitarity and analiticity [7]. A single, isolated exotic pole $\pi_1$, compatible with the Lattice QCD [3] suggestions is obtained in the $\ell = 1$ partial wave. Its mass and width are determined to be $1564 \pm 24 \pm 86$ MeV and $492 \pm 54 \pm 102$ MeV, respectively, while two ordinary mesons $a_2(1320)$ and the $a_2'(1700)$ are found in the tensor partial wave. The systematic uncertainties are obtained through the modification of both parameters and functional forms of the parameterization.

A.R. wishes to thank the Excited QCD 2019 organizers for such a nice conference. This work was partially supported by the U.S. Department of Energy under grants No. DE-AC05-06OR23177 and No. DE-FG02-87ER 40365, and Ministerio de Ciencia, Innovación y Universidades (Spain) grant FPA2016-75654-C2-2-P. A.R. would like to acknowledge the Universidad Complutense of Madrid for a predoctoral fellowship.

## REFERENCES

[1] B. Ketzer, *PoS* **QNP2012**, 025 (2012); C.A. Meyer, E.S. Swanson, *Prog. Part. Nucl. Phys.* **82**, 21 (2015); A. Esposito, A. Pilloni, A.D. Polosa, *Phys. Rep.* **668**, 1 (2016).

[2] D. Horn, J. Mandula, *Phys. Rev. D* **17**, 898 (1978); N. Isgur, J.E. Paton, *Phys. Rev. D* **31**, 2910 (1985); M.S. Chanowitz, S.R. Sharpe, *Nucl. Phys. B* **222**, 211 (1983) [*Erratum ibid.* **228**, 588 (1983)]; A.P. Szczepaniak, E.S. Swanson, *Phys. Rev. D* **65**, 025012 (2002); S.D. Bass, E. Marco, *Phys. Rev. D* **65**, 057503 (2002).

[3] P. Lacock *et al.* [UKQCD Collaboration], *Phys. Lett. B* **401**, 308 (1997); C.W. Bernard *et al.* [MILC Collaboration], *Phys. Rev. D* **56**, 7039 (1997); J.J. Dudek *et al.* [Hadron Spectrum Collaboration], *Phys. Rev. D* **88**, 094505 (2013).

[4] M. Aghasyan *et al.* [COMPASS Collaboration], *Phys. Rev. D* **98**, 092003 (2018).

[5] M. Alekseev *et al.* [COMPASS Collaboration], *Phys. Rev. Lett.* **104**, 241803 (2010).

[6] C. Adolph *et al.* [COMPASS Collaboration], *Phys. Lett. B* **740**, 303 (2015).

[7] A. Rodas *et al.* [JPAC Collaboration], *Phys. Rev. Lett.* **122**, 042002 (2019).

[8] A. Jackura *et al.* [JPAC and COMPASS collaborations], *Phys. Lett. B* **779**, 464 (2018).

[9] R.T. Deck, *Phys. Rev. Lett.* **13**, 169 (1964).

[10] G. Ascoli *et al.*, *Phys. Rev. D* **9**, 1963 (1974).